ELSEVIER

Powder Technology 104 (1999) 68–74

POWDER TECHNOLOGY

Influence of physical and interfacial characteristics on the wetting and spreading of fluids on powders

Laura L. Popovich [a,1], Donald L. Feke [a], Ica Manas-Zloczower [b,*]

[a] *Department of Chemical Engineering, Case Western Reserve University, Cleveland, OH 44106, USA*
[b] *Department of Macromolecular Science, Case Western Reserve University, Cleveland, OH 44106, USA*

Received 20 July 1998; received in revised form 18 January 1999; accepted 18 January 1999

Abstract

The wetting and spreading of liquid on compacts of carbon black and silica powders has been studied with the aim of investigating the degree to which the physical properties and chemical nature of the fluid govern the phenomena. Wetting experiments were performed with six fluids (glycerin, ethylene–propylene copolymer, squalene, poly(dimethylsiloxane), 1-butanol, and water) selected to provide a range of interfacial chemistries. The viscosity of these fluids spanned a range of three orders of magnitude. Capillary rise experiments gave insight into the wetting phenomena that occur between powders and large quantities of fluid. The observed infiltration kinetics was found to exhibit a different sensitivity to the fluid viscosity than what is explicitly predicted by the conventional Washburn analysis. This deviation is attributed to variation in the degree of saturation of the powder compacts arising from differences in viscosity of the infiltrating liquid. The wetting of compacts by small amounts of fluid was studied by contacting single drops of fluid onto carbon black compacts. Observed spreading and infiltration rates indicate that the wetting phenomena cannot be predicted on the basis of a simple balance between capillary and viscous forces. Cracking and microstructural rearrangement within powder compacts driven by the infiltrating liquid were also observed. The nature of this rearrangement was found to be strongly correlated with the kinetics of the wetting process.

Keywords: Interfacial characteristics; Permeability; Wetting and spreading

1. Introduction

In many technologies that involve finely divided particulate solids, the processing goal is manipulation of the size of the units into which the particles are clustered. Dispersion processes, for example, are concerned with the fragmentation of powder agglomerates and distribution of the small fragments or individual particles throughout a liquid medium. Dispersion processes are often encountered in the manufacture of filled or pigmented polymers, the fabrication of ceramic monoliths and composites, and the formulation of suspensions used for coating purposes. Since the ultimate properties of the final material are strongly affected by the quality of dispersion, there has been much research devoted to studying the factors that govern dispersion [1–4].

In other technologies, the formation of granules of powder or the consolidation of particle agglomerates are the processing goals. Such processes are practised in order to enhance the mechanical strength of agglomerates or improve the safety of handling the powdered materials. In such processes, small amounts of liquids are often used to bind the agglomerates together. The interaction of the binder liquid with the surface of the solids strongly affects the nature and kinetics of granulation or consolidation processes.

In both dispersion and consolidation processes, the wetting and spreading of liquids over the surface of powder particles play a critical role. Wetting involves the displacement of one fluid from the surface of the solid by another. In the case of agglomerates, wetting additionally involves filling the pore space. Although relatively large quantities of liquid are used in dispersion and smaller quantities are used in the granulation process, the same set of forces governs wetting in both cases.

In general, three types of wetting processes have been identified: adhesion, immersion, and spreading [5–7]. The work of adhesion (W_a) characterizes the free energy change per unit area associated with contacting a fluid with a

* Corresponding author.
[1] Current address: Motorola, Phoenix, AZ, USA.

0032-5910/99/$ - see front matter
PII: S0032-5910(99)00030-3

solid. The energy change associated with completely immersing a solid into a liquid is related to the work of immersion (W_i). Finally, the free energy change associated with the spreading of a liquid over the surface of a solid is the work of spreading (W_s). From consideration of the surface energies involved in the various wetting processes, it can be readily shown that the various wetting phenomena can be associated with the liquid–vapor surface tension (γ_{lv}) and contact angle (θ). These expressions are:

$$W_a = \gamma_{lv}(\cos\theta + 1) \quad (1)$$

$$W_i = \gamma_{lv}\cos\theta \quad (2)$$

$$W_s = \gamma_{lv}(\cos\theta - 1) \quad (3)$$

By convention, spontaneous processes are associated with positive (or nonnegative) values of the work of wetting given in Eqs. (1)–(3). Thus, fluid will stick to a solid ($W_a > 0$) if $\theta < \pi$, a particle will spontaneously be incorporated into a liquid ($W_i > 0$) if $\theta < \pi/2$, and fluid will continuously spread over a solid ($W_s = 0$) only if $\theta = 0$. Although the contact angle can be readily measured for liquids present on ideal smooth surfaces, there are many questions associated with the measurement of contact angle on powders due to the inherent surface roughness of particles and the pore structure of powder compacts. Nevertheless, the concept of a contact angle still remains useful for the characterization of wetting of powders.

The surface tension and contact angle also affect the kinetics of liquid incorporation into the pores of agglomerates and powder compacts. The capillary pressure (P_c) provides the driving force for the transport of liquids into agglomerates or powder compacts. From analysis of the wetting of an ideal cylindrical pore of radius r_p, the capillary pressure is

$$P_c = \frac{2\gamma_{lv}\cos\theta}{r_p} \quad (4)$$

The objective of this work is to enhance the understanding of some fundamental factors that govern agglomerate dispersion and powder consolidation processes and to test the limits of applicability of the conventional theory of wetting kinetics. Specifically, we investigate various aspects of how the fluid viscosity and interfacial chemistry influence the wetting of particles and the incorporation of fluids into particle compacts. Using carbon black and silica powders and several test fluids chosen to provide a range of properties, we analyze the rate of fluid movement into powder compacts using two methods. The first was a capillary rise technique in which the penetration of fluid into a powder compact was observed. The second method involved observation of the imbibition of a single drop of fluid into a powder compact. In the first case, a large reservoir of fluid supplies the wetting process while in the latter case, only a small volume of fluid participates in the wetting.

Table 1
Selected powder properties

Powder	S_{BET} (m^2/g)	ρ_{solid} (g/cm^3)	Chemistry
Monarch 900	205	1.86	Nonpolar
Silica	300	2.2	Polar

Table 2
Selected fluid properties

Fluid	ρ (g/cm^3)	γ (g/s^2)	η (g/cm s)	Chemistry
Glycerin[a]	1.26	63.10	9.34	Polar
Ethylene–propylene[b]	0.83	28.58	4.0	Nonpolar
Squalene[c]	0.86	31.85	0.118	Nonpolar
PDMS[d]	0.97	20.1	0.093	Slightly Polar
1-Butanol[a]	0.81	24.20	0.027	Polar
Water[a]	1.0	72.8	0.00898	Polar

[a] Ref. [8].
[b] Reported by manufacturer, Uniroyal Chemical.
[c] Reported by supplier, Sigma.
[d] Reported by manufacturer, Dow Corning.

2. Experimental

2.1. Materials

The carbon black used in this study was Monarch® 900, provided by the Cabot. This material is known as a low-structure black due to the fairly compact structure of the individual carbon black units. The silica used was Aerosil 300, a fumed, amorphous silica, provided by Rhone–Poulenc. These two powders were chosen because of their widespread use as fillers and because of their different chemistries and morphologies. The BET surface area and density of the solids are listed in Table 1.

The fluids used in this research were chosen in order to provide a range of surface tensions and chemistries. Table 2 shows the fluids used and some of their properties. In this and all of the succeeding tables, the fluids are entered in the order of highest to lowest viscosity. The polydimethylsiloxane, PDMS, was provided by Dow Corning. The ethylene–propylene copolymer was provided by Uniroyal Chemical. All other liquids were laboratory grade materials provided by Fisher Scientific or Sigma.

Contact angle measurements were performed using the sessile drop method of Heertjes and Kossen [9]. In this procedure, the contact angle made by a drop of liquid with a pressed compact of powder is calculated from a measurement of the droplet height.

2.2. Procedures

2.2.1. Capillary rise experiments

The apparatus for the capillary rise experiments consisted of a beaker containing 80 ml of liquid as a reservoir

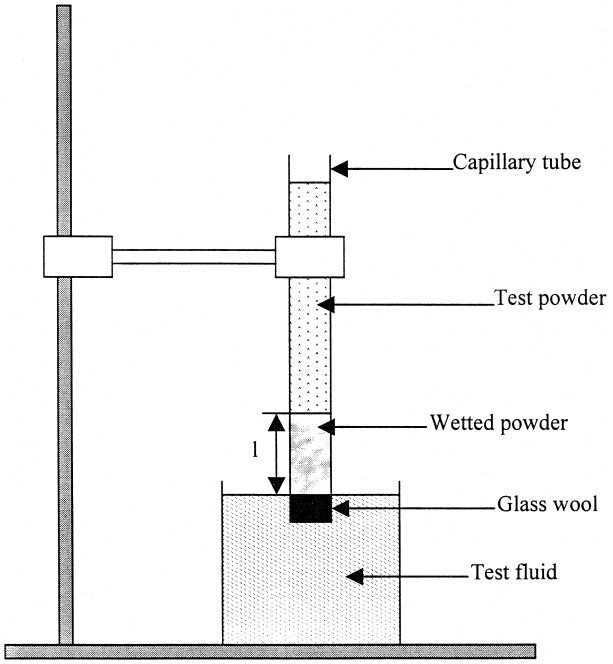

Fig. 1. Experimental setup for capillary rise.

and a vertical cylinder with graduated marks supported by a clamp. The cylinder was a 10-ml volumetric pipette with the bottom tip cut off. Glass wool was packed into the bottom of the tube to act as a support for the powder bed. The tube was then filled with a known mass of powder that had been dried at 100°C under vacuum for no less than 24 h. The carbon black was tapped to an average density of 0.29 g/cm^3 and the silica was tapped and then pressed to an average density of 0.16 g/cm^3. The capillary cylinder was then lowered into the beaker and time zero was recorded when the liquid first met the powder. The height of liquid drawn into the powder bed was recorded as volume vs. time for at least a 30-min period. Penetration distance was calculated directly from the recorded volumetric data. Only relatively short heights were achieved, and so the effect of gravity on the infiltration was neglected. Fig. 1 illustrates the experimental apparatus.

2.2.2. Drop–penetration experiments

Drop–penetration experiments were performed with carbon black only as it proved to be too difficult to prepare silica compacts with sufficient packing density to give rates of fluid penetration slow enough to measure. The carbon black was first dried for at least 24 h under vacuum and then compressed into flat compacts that gave an average density of 0.35 g/cm^3. Using a microsyringe, a droplet of fluid (typically 5 μl) was placed on the powder compact. Experiments involving the ethylene–propylene copolymer and glycerin used volumes of 25 μl since the high viscosity of these fluids precluded the use of the microsyringe to deliver a 5-μl droplet. A schematic of this setup is provided in Fig. 2.

Using a CCD camera and an image analysis system, the imbibition process was recorded and quantified. From above, the droplets appeared as circular shapes whose radii changed over the course of time as the fluid spread on, and penetrated into, the compact. Parameters that were measured included the radius of the fluid drop immediately after it was placed on the compact, the maximum size to which the droplet spread during the spreading process, and the time required for the droplet to be completely incorporated into the compact.

3. Results and discussion

3.1. Capillary rise experiments

The classical Washburn equation gives the rate of fluid infiltration into a powder compact. In differential form,

$$\frac{\mathrm{d}(l^2)}{\mathrm{d}t} = \frac{K_r \gamma_{lv} \cos\theta}{\eta} \tag{5}$$

where l is the length of infiltrated liquid up the capillary, t is the time of infiltration, η is the viscosity of the fluid,

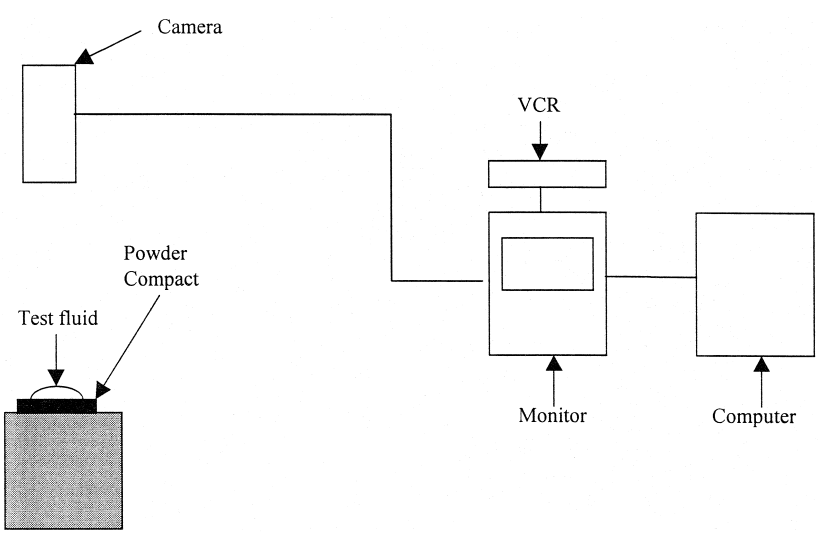

Fig. 2. Experimental setup for measurements of drop spreading.

Table 3
Values of W (10^{-6} cm) obtained from the capillary rise experiments

Fluids	Monarch 900	Silica
Glycerin	7.48 ± 0.50	6.25 ± 0.83
Ethylene–propylene	5.75 ± 1.9	4.74 ± 0.47
Squalene	4.85 ± 0.47	4.11 ± 0.41
PDMS	5.01 ± 0.31	3.26 ± 0.31
1-Butanol	2.96 ± 0.51	2.33 ± 0.15
Water	0.0461 ± 0.0063	1.26 ± 0.02

and $K_r = 4k/r_p$ (with k being the permeability and r_p being the average pore radius) is a parameter characterizing the structure of the compact [10]. Some restrictions apply when using this form: (i) pseudo-steady-state flow, (ii) no slip of the fluid along the pore wall, (iii) no externally applied pressure, and (iv) negligible influence of gravity. For a powder bed whose structure is unaffected by a passing fluid, Eq. (5) predicts that a plot of l^2 vs. t should be linear. The experimental data indeed followed this trend.

In order to isolate known and experimentally measurable quantities from parameters that characterize the solid or solid–liquid interaction, we rewrite Eq. (5) as

$$W \equiv \frac{\mathrm{d}(l^2)}{\mathrm{d}t}\frac{\eta}{\gamma_{lv}} = K_r \cos\theta \tag{6}$$

Here W is a lumped parameter that characterizes the wetting kinetics for the solid–liquid system. Table 3 reports values of W for experiments involving both carbon black and silica. It should be noted that when the carbon black–butanol trials were run, the powder compact seemed to collapse soon after the experiments were started. However, the data from the first 15 min gave linear results, and this information was used to calculate the W reported in Table 3.

The nonpolar fluids were expected to give larger values of W for the carbon black powder, and the polar fluids were expected to give larger W values with the silica powder. However, the trends in the observed wetting parameters were the same for both carbon black and silica (recognizing that to within experimental uncertainty, the results for PDMS and squalene on carbon black are indistinguishable).

Our measurements of the contact angle for the various fluids on carbon black compacts showed that the observed wide variations in W cannot be accounted for by differences in contact angle. Thus, the results shown in Table 3 suggest that there must be some variation in the structure parameter K_r induced by the wetting process. However, with the one exception noted above, no gross changes in the structure of the powder bed were observed.

It is interesting to note that the ordering of W for the various fluids matches the order of the fluid viscosity. This result suggests that fluid viscosity plays a different role in the wetting of a powder bed than is predicted explicitly by the Washburn analysis. This unpredicted dependence of infiltration kinetics on viscosity prevents explicit examination of the role of interfacial interactions on the wetting phenomena for this set of fluids.

The permeability of a porous medium at full saturation is a function of only its structure, and hence the value of K_r would be independent of the nature of the fluid if full saturation is achieved. However, wetting may be expected to yield less than 100% saturation, as some residual air will inevitably remain trapped inside the bed [9]. The actual degree of saturation achieved will depend on how well the fluid wets the solid and how the infiltration occurred. Consequently, the variation in K_r can give insight into how fluids saturate powder compacts. The permeability of a powder compact depends on some power (σ) of the saturation (S). Thus K_r can be expressed as

$$K_r = \frac{4k_{exp}}{r_p} = \frac{4k_{sat}S^{\sigma}}{r_p} \tag{7}$$

where k_{sat} would be the permeability if the compact was fully saturated. The value of σ for most porous media has been shown to range between 3 and 4 [11]. The results shown in Table 3 suggest that the higher the viscosity of the wetting fluid, the higher the level of saturation that will be achieved. Although higher viscosity fluids take longer to infiltrate the compact, this apparently results in a greater opportunity to fill a greater fraction of the pore space. The lower viscosity fluids rise very quickly, apparently entrapping more air in the process.

3.2. Drop–penetration experiments

After the liquid droplets were placed on the carbon black compounds, the droplets tended to spread outward as they were simultaneously drawn into the powder compact. Eventually, all of the liquid is drawn into the compact, and

Table 4
Initial (R_i) and maximum (R_m) radii of droplets, average rates of spread, and time of fluid penetration for carbon black compacts

Fluid	Volume (μl)	R_i (μm)	R_m (μm)	R_{spread} (μm/s)	t_m (s)
Glycerin	25	3041 ± 81	4456 ± 37	40.9 ± 1.0	237 ± 11
Ethylene–propylene	25	3026 ± 247	5858 ± 346	5.79 ± 1.37	1960 ± 112
Squalene	5	2463 ± 37	2870 ± 66	98.0 ± 9.8	28.8 ± 2.4
PDMS	5	2351 ± 18	2745 ± 21	65.2 ± 2.5	27.3 ± 0.9
1-Butanol	5	2861 ± 64	3304 ± 60	225 ± 21	6.75 ± 0.78
Water	5	1996 ± 17	2299 ± 28	40.6 ± 0.3	12.5 ± 0.4

in some cases, shifts in the structure or cracking of the wetted region could be seen.

Table 4 reports typical values of the initial radius of the fluid droplets placed on the powder compact, the maximum radius to which the drops spread, and the average rates of spread of the fluid drops. These were computed by taking the maximum drop radius less the initial drop radius, divided by the time required for the droplet to spread to its maximum radius. The total penetration times (t_m) defined to be the time it took for all the liquid to be incorporated within the powder compact is also given in Table 4. In contrast to the wetting rates observed in the capillary rise experiments, the trends of the drop penetration rates do not show a direct correlation with fluid viscosity.

Some interesting structural changes in the powder compacts were observed to result from the droplet penetration process. Fig. 3 depicts schematically some of the observed structural changes. Penetration of drops of butanol and the ethylene–propylene copolymer showed two different behaviors. These fluids either severely cracked (Fig. 3a) the wetted areas or cracked the areas into large chips (Fig. 3b). Squalene and PDMS also produced two behaviors, producing large chips (like those seen with butanol and the ethylene–propylene copolymer) or forming single flakes. Drops of water on carbon black also resulted in single chips, but no signs of cracking were ever seen. These chips could be easily lifted from the powder compact (Fig. 3c). In the case of glycerin, the wetted region shrank and sunk into the compact (Fig. 3d).

The cracking behavior, droplet radii, rates of spread, and total penetration times all provide information on the wetting of compacts by single drops. In order to provide a framework in which to analyze the relative effects of the governing parameters, we examine the dimensionless groups that govern the process. The balance of the surface tension forces driving infiltration and the viscous forces retarding it are described in terms of the Capillary number, Ca,

$$\mathrm{Ca} = \frac{\eta V}{\gamma_{lv}} \tag{8}$$

Here, V is characteristic fluid velocity, which for our purposes is assumed to be related to a characteristic length scale of the droplet divided by a characteristic time t_0. The form of Eq. (8) suggests that a characteristic time for the droplet penetration process (t_0) is

$$t_0 = \frac{\eta V_{drop}}{\gamma_{lv} A_{drop} \varepsilon S} \tag{9}$$

where V_{drop} is the volume of the drop used, A_{drop} is the area of the compact surface occupied by the droplet, ε is the compact porosity, and S is the degree of fluid saturation.

The degree of fluid saturation could be directly determined by testing the chips and flakes that formed from the penetration of the fluid drops into the compacts. The degree of saturation was calculated by first measuring the collective mass of the flakes, m_{flake}. The mass of powder in the flakes, m_p, was found from

$$m_p = m_{flake} - V_{drop}\,\rho_{fluid} \tag{10}$$

where ρ_{fluid} is the density of the fluid. In using Eq. (10), we assume that the total volume of liquid present in the original drop resides in the recovered fragments. Based on the known density of the compact (ρ_c), and the solid density of the carbon black powder ($\rho_p = 1.86$ g/cm^3), the volume of available pore space is given by

$$V_{pores} = \frac{m_p}{\rho_c} - \frac{m_p}{\rho_p} \tag{11}$$

Table 5
Degrees of saturation (S), characteristic times, and dimensionless penetration times for the carbon black compacts

Fluid	S	t_o (s)	$t^* = t_m / t_o$
Glycerin	0.536 ± 0.025	1.33e−02	1.78e+04
Ethylene–propylene	0.425 ± 0.033	9.27e−03	2.11e+04
Squalene	0.481 ± 0.059	1.75e−04	1.65e+05
PDMS	0.483 ± 0.065	1.46e−04	1.11e+05
1–Butanol	1	2.09e−05	3.24e+05
Water	0.423 ± 0.031	1.11e−05	1.12e+06

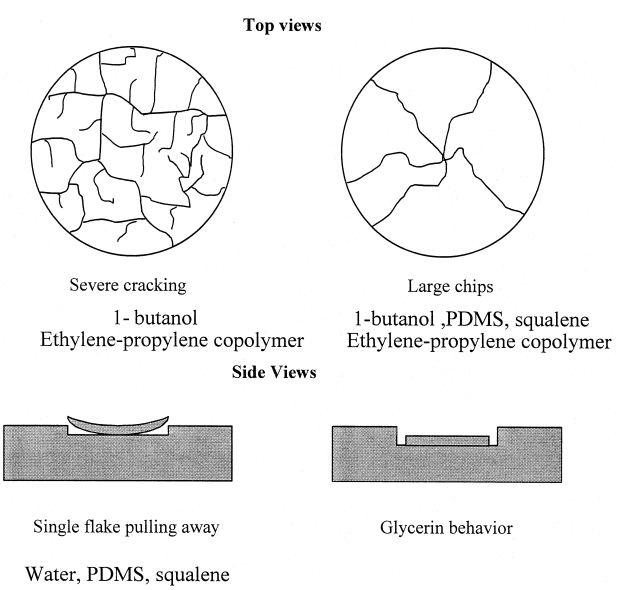

Fig. 3. Structural changes observed for carbon black compacts.

Then, the degree of saturation is given by

$$S = \frac{V_{\text{fluid}}}{V_{\text{pores}}} \quad (12)$$

Table 5 shows the values of S calculated using this approach. In the case of butanol, the calculation gave a value of S greater than one, which indicated that some of the butanol from the original droplet was not recovered in the flakes. Consequently, the saturation value for butanol was assigned to be one. These results give insight into the interfacial interactions occurring during the wetting process. Carbon black powders commonly contain a variety of secondary species [12,13]. During processing, groups made of heteroatoms, such as hydrogen and oxygen can become part of the carbon black surface and contribute to interfacial interactions. Such a powder can interact with both polar and nonpolar fluids. The saturation results indicate that butanol and glycerin, both of which contain organic backbones plus a polar functional group, gave the largest values of S. PDMS, being slightly polar showed the next greatest saturation value. The pure hydrocarbons squalene and the ethylene–propylene copolymer yielded even lower saturation values. Water, which has no organic character, gave the lowest degree of saturation.

Using the computed saturation values, the characteristic times for the droplet penetration experiments were calculated from Eq. (9) and are also presented in Table 5. These characteristic times can be used to present the experimentally measured penetration times in dimensionless form. The dimensionless penetration times t^* (calculated by dividing t_m by t_0), are also shown in Table 5. If the simple balance between capillary and viscous forces characterizes the droplet penetration process and the structure of the compact is the same in all cases, then the dimensionless penetration times should be the same for all fluids. However, since this is not the case, there are other factors, possibly the observed differences in cracking and flaking phenomena, which contribute to the differences in the dimensionless penetration times. It is interesting to note that the dimensionless penetration times roughly follow an inverse trend with the viscosity of the fluids.

To compare these results further, we recognize that the penetration of water apparently resulted in the least amount of structural rearrangement. For convenience, we normalize the dimensionless penetration time for each fluid relative to that for water. These normalized values are plotted as a function of a normalized fluid viscosity in Fig. 4. Included in this figure are comments about the structural changes associated with the penetration of the particular fluids. A strong correlation between the normalized dimensionless times and fluid viscosity is evident. Also, it is clear that the degree of structural rearrangement is more pronounced with increasing fluid viscosity. A simple physical explanation for this result can be offered.

As fluid enters the pores of a compact, capillary forces develop. These forces can act both on the fluid and on the particles forming the pores. With low viscosity fluids, the fluids can readily flow in response to these forces. However, higher viscosity fluids offer increased resistance to the fluid movement, and in these cases there can be a greater opportunity for particles to move in response to the capillary forces. Thus, as a high viscosity fluid penetrates a pore, the particles constituting the sides of that pore may be pulled inward in some regions, thereby forming cracks in other portions of the compact. For the case of the glycerin, the fluid infiltration moves the particles to such an extent that the entire wetted area collapses and no cracks are seen.

This explanation also applies to the capillary rise experiments. The rearrangement of the particles causes larger pores, which makes infiltration easier by creating preferred

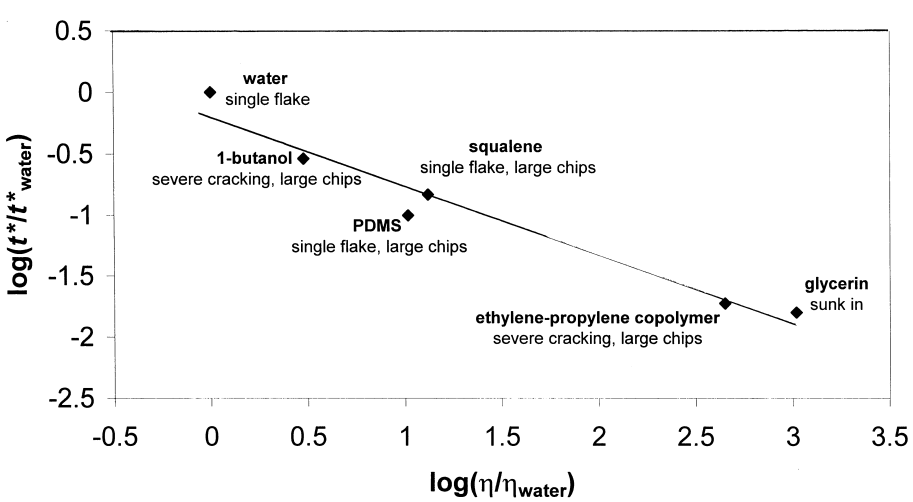

Fig. 4. Normalized dimensionless penetration time vs. normalized viscosity.

pathways for the fluid to move through. The increased ease of infiltration is reflected in the rate of fluid movement up the packed bed, explaining why the trends in the W values for both carbon black and silica correlate with the fluid viscosity.

4. Conclusions

The wetting data from the capillary rise experiments exhibited a different dependence on fluid viscosity than that predicted by the standard Washburn analysis. Thus, we were not able to directly examine the sensitivity of wetting to interfacial interactions. For the drop penetration experiments, the degree of fluid saturation indicated that the infiltration of the fluids into the powders could be explained by the presence of multiple types of functional groups on the carbon black surface. The calculation of the dimensionless penetration times indicated that the infiltration process was governed by more than a balance of capillary and viscous forces. Observations of microstructural rearrangement induced by the wetting leads to the conclusion that this is a significant factor in governing wetting and spreading by small amounts of fluid. The tendency for microstructural rearrangement could be correlated with the viscosity of the wetting fluid.

Acknowledgements

The authors are thankful to Cabot for partial support of this work. The authors also wish to acknowledge the financial support of the National Science Foundation through Grant CTS-9402682.

References

[1] F. Bohin, I. Manas-Zloczower, D.L. Feke, Kinetics of dispersion for sparse agglomerates in simple shear flows: application to silica agglomerates in silicone polymers, Chem. Eng. Sci. 51 (23) (1996) 5193–5204.
[2] Q. Li, D.L. Feke, I. Manas-Zloczower, Rubber Chem. Technol. 68 (1995) 836.
[3] H. Yamada, I. Manas-Zloczower, D.L. Feke, Influence of matrix infiltration on the dispersion kinetics of carbon black agglomerates, Powder Technol. 92 (1997) 163–169.
[4] H. Yamada, I. Manas-Zloczower, D.L. Feke, The influence of matrix viscosity and interfacial properties on the dispersion kinetics of carbon black agglomerates, Rubber Chem. Technol. 71 (1998) 1–16.
[5] C.K. Schoff, Modern Approaches to Wettability: Theory and Application, in: M.E. Schrader, G.I. Loeb (Eds.), Plenum, New York, 1992.
[6] G.D. Parfitt, Dispersion of Powders in Liquids with Special Reference to Pigments, 3rd edn., in: G.D. Parfitt (Ed.), Applied Science Publishers, NJ, 1981.
[7] N.W.F. Kossen, P.M. Heertjes, Chem. Eng. Sci. 20 (1964) 593.
[8] R.C. Weast (Ed.), CRC Handbook of Chemistry and Physics, 66th edn., CRC Press, Boca Raton, 1986.
[9] P.M. Heertjes, N.W.F. Kossen, Powder Technol. 1 (1967) 33.
[10] R.E. Ayala, E.Z. Casassa, G.D. Parfitt, Powder Technol. 51 (1987) 3.
[11] Th. Dracos, Modelling and Applications of Transport Phenomena in Porous Media, in: J. Bear, J.-M. Buchlin (Eds.), Kluwer Academic Publishers, Boston, 1987.
[12] J.A. Ayala, W.M. Hess, A.O. Dotson, G.A. Joyce, Rubber Chem. Technol. 63 (1994) 17.
[13] R.H. Bradley, I. Sutherland, E. Sheng, J. Colloid Interface Sci. 179 (1996) 561.